$B_s \to \gamma\gamma$ decay in model III and 3HDM(O_2) with CP violating effects.

M. Boz *
Physics Department, Hacettepe University
Ankara, Turkey

E. O. Iltan †
Physics Department, Middle East Technical University
Ankara, Turkey

Abstract

We analyse the CP asymmetry for $B_s \to \gamma\gamma$ in the two Higgs doublet model with tree level flavor changing currents (model III) and three Higgs doublet model with O_2 symmetry in the Higgs sector, including O_7 type long distance effects. Further, we study the dependencies of the branching ratio $Br(B_s \to \gamma\gamma)$ and the ratio of CP-even and CP-odd amplitude squares, $R = |A^+|^2/|A^-|^2$, on the CP parameter $sin\,\theta$. We found that, there is a weak CP asymmetry, at the order of 10^{-4}. Besides, the branching ratio $Br(B_s \to \gamma\gamma)$, and also R ratio, is not sensitive to the CP parameter for $|\frac{\bar{\xi}^U_{N,tt}}{\bar{\xi}^D_{N,bb}}| < 1$.

*E-mail address: mugeboz@thep1.hun.edu.tr
†E-mail address: eiltan@heraklit.physics.metu.edu.tr

1 Introduction

One of the most important classes of decays are rare B-meson decays which are induced by flavor changing neutral currents (FCNC) at loop level in the Standard Model (SM). Therefore, one can obtain quantitative information for the SM parameters , such as Cabbibo-Kobayashi-Maskawa (CKM) matrix elements, leptonic decay constants, CP ratio, etc. and the measurement of physical quantities like branching ratio (Br), CP asymmetry (A_{CP}),... etc, gives important clues about the model under consideration. These decays are also sensitive to the physics beyond the SM, such as two Higgs Doublet model (2HDM), Minimal Supersymmetric extension of the SM (MSSM) [1].

$B_s \rightarrow \gamma\gamma$ decay, which is an example of the rare B meson decays, is an important candidate to test the theoretical models and to construct new models in the framework of the planned experiments at the upcoming KEK and SLAC-B factories and existing hadronic accelerators. $B_s \rightarrow \gamma\gamma$ decay, induced by the process $b \rightarrow s\gamma\gamma$ in the quark level, has been studied in the SM [2]-[5] and 2HDM [6] without QCD corrections. Since the QCD corrections to the inclusive decay $b \rightarrow s\gamma$ are large (see [7] - [10] and references therein), it is expected that they are also large in the inclusive $b \rightarrow s\gamma\gamma$ decay and, therefore, in the exclusive $B_s \rightarrow \gamma\gamma$ decay. With the addition of the leading logarithmic (LLog) QCD corrections, the analysis has been repeated in the SM [11]-[13], 2HDM [14], MSSM [15] , and the strong sensitivity to these corrections was obtained. Recently, $B_s \rightarrow \gamma\gamma$ decay has been calculated in the framework of model III [16] with the addition of the LLog QCD corrections and the current upper limit of the Br ratio $Br(B_s \rightarrow \gamma\gamma) \leq 1.48\,.10^{-4}$ [17] was theoretically obtained for larger values of the Yukawa coupling $\bar{\xi}_{N,bb}$ and the ratio $|r_{tb}| = |\frac{\bar{\xi}_{N,tt}}{\bar{\xi}_{N,bb}}| >> 1$ (see Appendix C for definitions).

In the present work, we study $B_s \rightarrow \gamma\gamma$ decay in 2HDM (model III) and three Higgs doublet model with O_2 symmetry in the Higgs sector ($3HDM(O_2)$) [18], with complex Yukawa couplings. In our calculations, we take into account the perturbative QCD corrections in the LLog approximation by following a method based on heavy quark effective theory (HQET) for the bound state of the B_s meson [11] and we also consider the long-distance effects due to the process $B_s \rightarrow \phi\gamma \rightarrow \gamma\gamma$, [11]. Since the complex Yukawa couplings are chosen in the calculations, in addition to the CKM matrix elements, there is a new source for CP violation. Using this new source, we obtain A_{CP} in model III at the order of 10^{-4}, which is a small effect. Furthermore, we calculate this quantity in the $3HDM(O_2)$ and find that there is a small decrease as compared to the former one for $\sin\theta \leq 0.5$. Finally, the calculations of Br and the CP ratio $R = |\frac{A^+}{A^-}|$ show that these physical quantities are not sensitive to the models

under consideration for $|r_{tb}| = |\frac{\bar{\xi}^U_{N,tt}}{\bar{\xi}^D_{N,bb}}| < 1$ (see Section 3).

The paper is organized as follows: In section 2, we present the LLog QCD corrected amplitude for the exclusive decay $B_s \rightarrow \gamma\gamma$ and the CP-even A^+ and CP-odd A^- amplitudes in a HQET inspired approach. Then, we calculate A_{CP}, assuming that the Yukawa couplings are complex in general and also derive Br. Finally, these calculations are repeated in the $3HDM(O_2)$ model with the redefinition of the Yukawa combination λ_θ (see eq. (20)). Section 3 is devoted to our analysis of the physical quantities under consideration and our conclusions. In the Appendix, we give a brief explanation about the model III and $3HDM(O_2)$ which we study. Further, we present the operator basis and the Wilson coefficients responsible for the inclusive $b \rightarrow s\gamma\gamma$ decay in the model III. Finally, we give the explicit forms of some functions appearing in the Wilson coefficients.

2 Leading logarithmic improved short-distance contributions in the model III for the decay $B_s \rightarrow \gamma\gamma$

The LLog corrected effective Hamiltonian in the model III (see Appendix A) for the exclusive $B_s \rightarrow \gamma\gamma$ decay is

$$\mathcal{H}_{eff} = -4\frac{G_F}{\sqrt{2}} V_{tb} V^*_{ts} \sum_i \left(C_i(\mu) O_i(\mu) + C'_i(\mu) O'_i(\mu) \right) \ , \tag{1}$$

where the O_i, O'_i are operators given in eqs. (41), (42), and C_i, C'_i are the Wilson coefficients renormalized at the scale μ. The Wilson coefficients C_i and C'_i can be calculated perturbatively and their explicit forms of at m_W level are presented in Appendix B. The effective Hamiltonian (1) is obtained by integrating out the heavy degrees of freedom, i.e , t quark, $W^\pm$, $H^\pm$, H_1, and H_2 bosons in the present case where $H^\pm$ denote charged, H_1 and H_2 denote neutral Higgs bosons. Further, QCD corrections are done through matching the full theory with the effective low energy theory at the high scale $\mu = m_W$ and evaluating the Wilson coefficients from m_W down to the lower scale $\mu \sim O(m_b)$. In our case, we choose the higher scale as $\mu = m_W$ since the evaluation from the scale $\mu = m_{H^\pm}$ to $\mu = m_W$ gives negligible contribution to the Wilson coefficients ($\sim 5\%$) since the charged Higgs boson is heavy due to the current theoretical restrictions (see [14], [19])

The decay amplitude for the $B_s \rightarrow \gamma\gamma$ decay is obtained by sandwiching the effective Hamiltonian between the B_s and two photon states, i.e. $< B_s|\mathcal{H}_{eff}|\gamma\gamma >$, and the matrix element can be written in terms of two Lorentz structures [5] - [6], [11]-[13]:

$$\mathcal{A}(B_s \rightarrow \gamma\gamma) = A^+ \mathcal{F}_{\mu\nu}\mathcal{F}^{\mu\nu} + i A^- \mathcal{F}_{\mu\nu}\tilde{\mathcal{F}}^{\mu\nu} \ , \tag{2}$$

where $\tilde{\mathcal{F}}_{\mu\nu} = \frac{1}{2}\epsilon_{\mu\nu\alpha\beta}\mathcal{F}^{\alpha\beta}$ and A^+ (A^-) is the CP-even (CP-odd) amplitude. Denoting CP-even (CP-odd) amplitude coming from the first operator set eq. (41) as A_1^+ (A_1^-) and the primed operator set eq. (42) as A_2^+ (A_2^-), in a HQET inspired approach, we get,

$$\begin{aligned}
A_1^+ &= \frac{\alpha_{em} G_F}{\sqrt{2}\pi}\frac{f_{B_s}}{m_{B_s}^2}\lambda_t \left(\frac{1}{3}\frac{m_{B_s}^4(m_b^{eff}-m_s^{eff})}{\bar{\Lambda}_s(m_{B_s}-\bar{\Lambda}_s)(m_b^{eff}+m_s^{eff})}C_7^{eff}(\mu)\right.\\
&- \left.\frac{4}{9}\frac{m_{B_s^2}}{m_b^{eff}+m_s^{eff}}\left[\,(-m_b J(m_b)+m_s J(m_s))D(\mu)-m_c J(m_c)E(\mu)\,\right]\right),\\
A_1^- &= -\frac{\alpha_{em} G_F}{\sqrt{2}\pi} f_{B_s}\lambda_t \left(\frac{1}{3}\frac{1}{m_{B_s}\bar{\Lambda}_s(m_{B_s}-\bar{\Lambda}_s)}g_- C_7^{eff}(\mu) - \sum_q Q_q^2 I(m_q) C_q(\mu)\right.\\
&+ \left.\frac{1}{9(m_b^{eff}+m_s^{eff})}\left[\,(m_b\triangle(m_b)+m_s\triangle(m_s))D(\mu)+m_c\triangle(m_c)E(\mu)\,\right]\right)\ , \qquad (3)
\end{aligned}$$

and,

$$\begin{aligned}
A_2^+ &= \frac{\alpha_{em} G_F}{\sqrt{2}\pi}\frac{f_{B_s}}{m_{B_s}^2}\lambda_t \left(\frac{1}{3}\frac{m_{B_s}^4(m_b^{eff}-m_s^{eff})}{\bar{\Lambda}_s(m_{B_s}-\bar{\Lambda}_s)(m_b^{eff}+m_s^{eff})}C_7^{\prime eff}(\mu)\right),\\
A_2^- &= -\frac{\alpha_{em} G_F}{\sqrt{2}\pi} f_{B_s}\lambda_t \left(\frac{1}{3}\frac{1}{m_{B_s}\bar{\Lambda}_s(m_{B_s}-\bar{\Lambda}_s)}g_- C_7^{\prime eff}(\mu)\right)\ , \qquad (4)
\end{aligned}$$

However, we do not take the CP-even and CP-odd amplitudes corresponding to the primed operator set since their contribution is small as compared to former ones (see [16, 20]). In eqs. (3) and (4), $Q_q = \frac{2}{3}$ for $q = u, c$ and $Q_q = -\frac{1}{3}$ for $q = d, s, b$. Here, we have used the unitarity of the CKM-matrix $\sum_{i=u,c,t} V_{is}^* V_{ib} = 0$, and also the contribution due to $V_{us}^* V_{ub} \ll V_{ts}^* V_{tb} \equiv \lambda_t$ is neglected. The function g_- is defined as [11]:

$$g_- = m_{B_s}(m_b^{eff}+m_s^{eff})^2 + \bar{\Lambda}_s(m_{B_s}^2 - (m_b^{eff}+m_s^{eff})^2)\ . \qquad (5)$$

The parameter $\bar{\Lambda}_s$ enters in eqs. (3) and (4) through the bound state kinematics (for details see [11]). In the expression (3), the LLog QCD corrected Wilson coefficients $C_{1\ldots10}(\mu)$ [11] - [13] are,

$$\begin{aligned}
C_u(\mu) &= C_d(\mu) = (C_3(\mu)-C_5(\mu))N_c + C_4(\mu) - C_6(\mu)\ ,\\
C_c(\mu) &= (C_1(\mu)+C_3(\mu)-C_5(\mu))N_c + C_2(\mu) + C_4(\mu) - C_6(\mu)\ ,\\
C_s(\mu) &= C_b(\mu) = (C_3(\mu)+C_4(\mu))(N_c+1) - N_c C_5(\mu) - C_6(\mu)\ ,\\
D(\mu) &= C_5(\mu) + C_6(\mu) N_c\ ,\\
E(\mu) &= C_{10}(\mu) + C_9(\mu) N_c \qquad (6)
\end{aligned}$$

and the effective coefficient $C_7^{eff}(\mu)$, defined in the NDR scheme, is [20]

$$\begin{aligned}
C_7^{eff}(\mu) &= C_7^{2HDM}(\mu) + Q_d\,(C_5^{2HDM}(\mu) + N_c\,C_6^{2HDM}(\mu))\ ,\\
&+ Q_u\,(\frac{m_c}{m_b}\,C_{10}^{2HDM}(\mu) + N_c\,\frac{m_c}{m_b}\,C_9^{2HDM}(\mu)) \qquad (7)
\end{aligned}$$

where N_c is the number of colours ($N_c = 3$ for QCD). The functions $I(m_q)$, $J(m_q)$ and $\triangle(m_q)$ come from the irreducible diagrams with an internal q type quark propagating and their explicit forms are given in Appendix D. In our numerical analysis we used the input values given in Table (1).

Parameter	Value
m_c	1.4 (GeV)
m_b	4.8 (GeV)
α_{em}^{-1}	129
λ_t	0.04
$\Gamma_{tot}(B_s)$	$4.09 \cdot 10^{-13}$ (GeV)
f_{B_s}	0.2 (GeV)
m_{B_s}	5.369 (GeV)
m_t	175 (GeV)
m_W	80.26 (GeV)
m_Z	91.19 (GeV)
$\Lambda_{QCD}^{(5)}$	0.214 (GeV)
$\alpha_s(m_Z)$	0.117
λ_2	0.12 (GeV^2)
λ_1	-0.29 (GeV^2)
$\bar{\Lambda}_s$	590 (MeV)
$\bar{\Lambda}$	500 (MeV)

Table 1: Values of the input parameters used in the numerical calculations unless otherwise specified.

At this stage, we will calculate the CP violating asymmetry for the given process. The possible sources of such effects are the complex Yukawa couplings in the model III. Here, we neglect all the Yukawa couplings except $\bar{\xi}^U_{N,tt}$ and $\bar{\xi}^D_{N,bb}$ (see Section 3). Using the expressions for the decay amplitude

$$\Gamma = \frac{1}{32\pi m_{B_s}}[4|A^+|^2 + \frac{1}{2} m_{B_s}^4 |A^-|^2] \tag{8}$$

and the CP-asymmetry

$$A_{CP} = \frac{\Gamma(B_s \to \gamma\gamma) - \Gamma(\bar{B}_s \to \gamma\gamma)}{\Gamma(B_s \to \gamma\gamma) + \Gamma(\bar{B}_s \to \gamma\gamma)} \;, \tag{9}$$

we get

$$A_{CP} = 2Im(\lambda_\theta) \, \frac{8Im(T_1^{(+)} T_2^{(+)*}) + m_{B_s}^4 Im(T_1^{(-)} T_2^{(-)*})}{D} \tag{10}$$

where

$$
\begin{aligned}
T_1^{(+)} &= aP_1 \\
T_2^{(+)} &= aP_2 + b \\
T_1^{(-)} &= cP_1 \\
T_2^{(-)} &= cP_2 + d
\end{aligned}
\tag{11}
$$

and

$$
\begin{aligned}
a &= \frac{\alpha_{em} G_F}{\sqrt{2}\pi} \frac{f_{B_s}}{3} \frac{m_{B_s}^2}{\bar{\Lambda}_s} \lambda_t \frac{(m_b^{eff} - m_s^{eff})}{(m_{B_s} - \bar{\Lambda}_s)(m_b^{eff} + m_s^{eff})} \\
b &= -\frac{\alpha_{em} G_F}{\sqrt{2}\pi} \frac{4 f_{B_s}}{9({m_b}^{eff} + {m_s}^{eff})} \lambda_t [(-m_b J(m_b) + m_s J(m_s)] D(\mu) - m_c J(m_c) E(\mu)] \\
c &= -\frac{\alpha_{em} G_F}{\sqrt{2}\pi} f_{B_s} \frac{1}{3 m_B \bar{\Lambda}_s (m_{B_s} - \Lambda_s)} \lambda_t \, g_- \\
d &= -\frac{\alpha_{em} G_F}{\sqrt{2}\pi} f_B \lambda_t [\sum_q Q_q^2 I(m_q) C_q(\mu) + \\
&\quad \frac{1}{9(m_b^{eff} + m_s^{eff})} \{(m_b \Delta(m_b) + m_s \Delta(m_s)) D(\mu) + m_c \Delta(m_c) E(\mu)\}\,]
\end{aligned}
\tag{12}
$$

In eq. (10), we used the parametrization,

$$
C_7^{eff}(\mu) = P_1(\mu) \lambda_\theta + P_2(\mu) \tag{13}
$$

with

$$
\lambda_\theta = \frac{1}{m_t m_b} |\bar{\xi}^U_{N,tt} \bar{\xi}^D_{N,bb}| e^{i\theta} \tag{14}
$$

Here, $\bar{\xi}^U_{N,tt}$ is chosen to be as real and $\bar{\xi}^D_{N,bb}$ as complex, namely $\bar{\xi}^D_{N,bb} = |\bar{\xi}^D_{N,bb}| e^{i\theta}$. Finally the functions $P_1(\mu)$ and $P_2(\mu)$, in the LLog approximation [21], are

$$
\begin{aligned}
P_1(\mu) &= \eta^{16/23} F_2(y) + \frac{8}{3}(\eta^{14/23} - \eta^{16/23}) G_2(y) \\
P_2(\mu) &= \eta^{16/23} [C_7^{SM}(m_W + \frac{|\bar{\xi}^U_{N,tt}|^2}{m_t^2} F_1(y)] \\
&\quad + \frac{8}{3}(\eta^{14/23} - \eta^{16/23}) [C_8^{SM}(m_W + \frac{|\bar{\xi}^U_{N,tt}|^2}{m_t^2} G_1(y)] \\
&\quad + Q_d (C_5^{LO}(\mu) + N_c C_6^{LO}(\mu)) + + Q_u (\frac{m_c}{m_b} C_{12}^{LO}(\mu) + N_c \frac{m_c}{m_b} C_{11}^{LO}(\mu)) \\
&\quad + C_2(m_W) \sum_{i=1}^{8} h_i \eta^{\alpha_i}
\end{aligned}
\tag{15}
$$

and

$$
\begin{aligned}
D &= |\lambda_\theta|^2\{8|T_1^{(+)}|^2 + m_{B_s}^4|T_2^{(-)}|^2\} + 2Re(\lambda_\theta)\{8Re(T_1^{(+)}T^{(+)*}) \\
&\quad + m_{B_s}^4 Re(T_1^{(-)}T^{(-)*})\} + \{8|T_2^{(+)}|^2 + m_{B_s}^4|T_2^{(-)}|^2\}
\end{aligned} \tag{16}
$$

In eq. 15, $\eta = \alpha_s(m_W)/\alpha_s(\mu)$ and h_i, a_i are numbers which appear during the evaluation of the Wilson coefficients [22].

Now, we would like to add the LD distance contributions due to the process $B_s \to \phi\gamma \to \gamma\gamma$ [11]. These effects can be taken into account by the redefinition of the functions $T_1^{(+)}, T_2^{(+)}, T_1^{(-)}, T_2^{(-)}$,

$$
\begin{aligned}
T_1^{\prime(+)} &= T_1^{(+)} + P_1\, a_{LD}^{(+)} \\
T_2^{\prime(+)} &= T_2^{(+)} + P_2\, a_{LD}^{(+)} \\
T_1^{\prime(-)} &= T_1^{(+)} + P_1\, a_{LD}^{(-)} \\
T_2^{\prime(-)} &= T_2^{(+)} + P_2\, a_{LD}^{(-)}
\end{aligned} \tag{17}
$$

where

$$
\begin{aligned}
a_{LD}^{(+)} &= -\sqrt{2}\frac{\alpha_{em}G_F}{\pi}\bar{F}_1(0) f_\phi(0)\lambda_t \frac{m_b(m_{Bs}^2 - m_\phi^2)}{3m_\phi m_{Bs}^2} \\
a_{LD}^{(-)} &= \sqrt{2}\frac{\alpha_{em}G_F}{\pi}\bar{F}_1(0) f_\phi(0)\lambda_t \frac{m_b}{3m_\phi}
\end{aligned} \tag{18}
$$

Note that there is also a LD contribution due to the chain process $B_s \to \phi\psi \to \phi\gamma \to \gamma\gamma$ and it is negligible compared to the one due to the decay $B_s \to \phi\gamma \to \gamma\gamma$ [23].

Finally, we derive the branching ratio for the given process as

$$
\begin{aligned}
Br &= \frac{1}{64\,\pi\, m_{B_s}\Gamma_{tot}}[\,|\lambda_\theta|^2\{8|T_1^{(+)}|^2 + m_{B_s}^4|T_1^{(-)}|^2\} + 4Re(\lambda_\theta)\{8T_1^{(+)}Re(T_2^{(+)}) \\
&\quad + m_{B_s}^4 T_1^{(-)} Re(T_2^{(-)})\} + \{8|T_2^{(+)}|^2 + m_B^4|T_2^{(-)}|^2\}\,]
\end{aligned} \tag{19}
$$

In the $3HDM(O_2)$(see Appendix C and [18]), the physical quantities under consideration are the same with the redefinition of λ_θ,

$$
\lambda_\theta = \frac{1}{m_t m_b}\bar{\epsilon}_{N,tt}^U \bar{\epsilon}_{N,bb}^D(\cos^2\theta + i\sin^2\theta) \tag{20}
$$

3 Discussion

In the model III, there are many parameters, such as complex Yukawa couplings, $\xi_{i,j}^{U,D}$ (i,j are flavor indices), masses of charged and neutral Higgs bosons and they should be restricted using

experimental results. All the Yukawa couplings except $\xi^U_{N,tt}$ and $\xi^D_{N,bb}$ are cancelled based on the experimental measurements by CLEO [24],

$$Br(B \to X_s \gamma) = (3.15 \pm 0.35 \pm 0.32)\, 10^{-4} \,, \tag{21}$$

$\Delta F = 2$ mixing and the ρ parameter [25] (see [20] for details). This discussion also allows us to neglect the contributions coming from the primed operator set. Further, the CP parameter "θ", appearing in the combination $\bar{\xi}^U_{N,tt}\bar{\xi}^{D*}_{N,bb} = |\bar{\xi}^U_{N,tt}\xi^D_{N,bb}| e^{-i\theta}$, is restricted due to the experimental upper limit on neutron electric dipole moment $d_n < 10^{-25}$ e.cm, which gives an upper bound to the combination $\frac{1}{m_t m_b} Im(\bar{\xi}^U_{N,tt}\bar{\xi}^{D*}_{N,bb}) < 1.0$ for $m_H \approx 200$ Gev [26].

Now, we are ready to start with the discussion of CP asymmetry in our process. Note that, in the analysis, $|C_7^{eff}|$ is allowed to lie in the region, $0.257 \leq |C_7^{eff}| \leq 0.439$ due to the CLEO measurement (see [20]) and the parameters $\bar{\xi}^U_{N,tt}$, $\bar{\xi}^D_{N,bb}$ and θ are restricted. We choose the scale as $\mu = \frac{m_b}{2}$ since we predict that this choice reproduce effectively the Next to Leading Order (NLO) result (see [11]).

In Fig 1(2), we plot the A_{CP} of the decay $B_s \to \gamma\gamma$ with respect to $\sin\theta$, for $\bar{\xi}^D_{N,bb} = 40\, m_b$ and $m_{H^\pm} = 400$ GeV, in the case where the ratio $|r_{tb}| = |\frac{\bar{\xi}^U_{N,tt}}{\bar{\xi}^D_{N,bb}}| < 1$, without (with) LD effects, in model III. A_{CP} is restricted in the region bounded by solid (dashed) lines for $C_7^{eff} > 0$ ($C_7^{eff} < 0$). Figures show that A_{CP} is at the order of 10^{-4}, which is a weak effect. A_{CP} is larger for $C_7^{eff} > 0$, as compared to the $C_7^{eff} < 0$ case and it is possible that A_{CP} vanishes and even take negative values for $\sin\theta > 0$ and $C_7^{eff} < 0$. Addition of LD effects enhances A_{CP} small in amount.

Fig 3(4) denotes the same dependence of A_{CP} for $3HDM(O_2)$ with (without) LD effects. The area of the restricted region and the possible values of A_{CP} are smaller as compared to the 2HDM case. For example, for $\sin\theta = 0.5$ and $C_7^{eff} > 0$, the upper limit of A_{CP} decreases by an amount of 50%. However, the order of A_{CP} still remains the same, namely 10^{-4}. Furthermore, A_{CP} is not sensitive to the charged Higgs boson mass $m_{H^\pm}$ (see Fig 5 and (6).

Figures 7-10 show the Br of the given process for the model III and $3HDM(O_2)$. In Fig 7 (8), we present the dependence of Br on $\sin\theta$ without(with) LD effects for $|r_{tb}| < 1$, in model III. The restricted region lies between solid (dashed) lines for $C_7^{eff} > 0$ ($C_7^{eff} < 0$). Note that Br for $C_7^{eff} < 0$ is greater than the one for $C_7^{eff} > 0$. It is observed that the enhancement of Br in the SM is negligible ($Br_{SM} = 3.45\, 10^{-7}$ with LD effects and $Br_{SM} = 4.71\, 10^{-7}$ without LD effects). Therefore model III can not be distinguished from the SM with the measurement of Br of the given process, for $|r_{tb}| < 1$. Fig 9 and (10 denote the same dependence for $3HDM(O_2)$ and the results are similar to the 2HDM case.

Finally, in Fig 11, we plot the CP ratio $R = |\frac{A^+}{A^-}|$ with respect to $\sin\theta$ for $2HDM$. Here, the solid line corresponds to $C_7^{eff} > 0$ and the dashed line to $C_7^{eff} < 0$. This figure shows that R is not sensitive to CP violating parameter θ and there is a small enhancement compared to the SM value ($R_{SM} = 0.845$). This ratio is also non-sensitive to the models under consideration.

For completeness, we would like to note that there are some uncertainities coming from the choice of the bound state parameters m_b^{eff}, $\bar{\Lambda}_s$ and the decay constant f_{B_s}. The physical quantities are sensitive to these parameters. For example, the larger m_b^{eff} (smaller $\bar{\Lambda}_s$), the larger Br, R and the smaller A_{CP}.

In conclusion, we study the CP asymmetry of $B_s \to \gamma\gamma$ decay in the framework of the model III and $3HDM(O_2)$. Further, we analyze the Br and R ratio of the given process. We can summarize the main points of our results:

- In model III, a weak A_{CP} is possible and it is at the order of 10^{-4}. This effect increases with the addition of LD contributions and this holds also in the $3HDM(O_2)$ model. The measurement of such a small value of A_{CP} can give information about the sign of C_7^{eff}.

- The Br ratio is not sensitive to CP violation parameter θ and the enhancement as compared to SM is negligible in both models, for $|r_{tb}| < 1$

- The R ratio is also non-sensitive to the parameter θ in both models.

A Appendix Model III

The Yukawa interaction for the 2HDM in the general case is

$$\mathcal{L}_Y = \eta^U_{ij}\bar{Q}_{iL}\tilde{\phi}_1 U_{jR} + \eta^D_{ij}\bar{Q}_{iL}\phi_1 D_{jR} + \xi^U_{ij}\bar{Q}_{iL}\tilde{\phi}_2 U_{jR} + \xi^D_{ij}\bar{Q}_{iL}\phi_2 D_{jR} + h.c. \ , \tag{22}$$

where L and R denote chiral projections $L(R) = 1/2(1 \mp \gamma_5)$, ϕ_i for $i = 1, 2$, are the two scalar doublets, $\eta^{U,D}_{ij}$ and $\xi^{U,D}_{ij}$ are the matrices of the Yukawa couplings. With the choice of ϕ_1 and ϕ_2 [25]

$$\phi_1 = \frac{1}{\sqrt{2}}\left[\left(\begin{array}{c} 0 \\ v + H^0 \end{array}\right) + \left(\begin{array}{c} \sqrt{2}\chi^+ \\ i\chi^0 \end{array}\right)\right] ; \phi_2 = \frac{1}{\sqrt{2}}\left(\begin{array}{c} \sqrt{2}H^+ \\ H_1 + iH_2 \end{array}\right) \ , \tag{23}$$

and the vacuum expectation values,

$$< \phi_1 >= \frac{1}{\sqrt{2}}\left(\begin{array}{c} 0 \\ v \end{array}\right) \ ; < \phi_2 >= 0 \ , \tag{24}$$

we can write the Flavor Changing (FC) part of the interaction as

$$\mathcal{L}_{Y,FC} = \xi^U_{ij}\bar{Q}_{iL}\tilde{\phi}_2 U_{jR} + \xi^D_{ij}\bar{Q}_{iL}\phi_2 D_{jR} + h.c. \ , \tag{25}$$

where the couplings $\xi^{U,D}$ for the FC charged interactions are

$$\begin{aligned} \xi^U_{ch} &= \xi_{neutral}\, V_{CKM} \ , \\ \xi^D_{ch} &= V_{CKM}\, \xi_{neutral} \ , \end{aligned} \tag{26}$$

and $\xi^{U,D}_{neutral}$ [1] is defined by the expression

$$\xi^{U,D}_N = (V^{U,D}_L)^{-1}\xi^{U,D}V^{U,D}_R \ . \tag{27}$$

Here, the charged couplings appear as a linear combinations of neutral couplings multiplied by V_{CKM} matrix elements.

B Appendix 3HDM(O_2)

In the 3HDM the general Yukawa interaction is,

$$\begin{aligned} \mathcal{L}_Y &= \eta^U_{ij}\bar{Q}_{iL}\tilde{\phi}_1 U_{jR} + \eta^D_{ij}\bar{Q}_{iL}\phi_1 D_{jR} + \xi^U_{ij}\bar{Q}_{iL}\tilde{\phi}_2 U_{jR} + \xi^D_{ij}\bar{Q}_{iL}\phi_2 D_{jR} \\ &+ \rho^U_{ij}\bar{Q}_{iL}\tilde{\phi}_3 U_{jR} + \rho^D_{ij}\bar{Q}_{iL}\phi_3 D_{jR} + h.c. \ , \end{aligned} \tag{28}$$

[1] In all next discussion we denote $\xi^{U,D}_{neutral}$ as $\xi^{U,D}_N$.

where ϕ_i for $i = 1, 2, 3$, are three scalar doublets and $\eta_{ij}^{U,D}$, $\xi_{ij}^{U,D}$, $\rho_{ij}^{U,D}$ are the Yukawa matrices having complex entries, in general. Now, we choose scalar Higgs doublets such that the first one describes only the SM part and last two carry the information about new physics beyond the SM:

$$\phi_1 = \frac{1}{\sqrt{2}} \left[\left(\begin{array}{c} 0 \\ v + H^0 \end{array} \right) + \left(\begin{array}{c} \sqrt{2}\chi^+ \\ i\chi^0 \end{array} \right) \right] ,$$
$$\phi_2 = \frac{1}{\sqrt{2}} \left(\begin{array}{c} \sqrt{2}H^+ \\ H^1 + iH^2 \end{array} \right) , \; \phi_3 = \frac{1}{\sqrt{2}} \left(\begin{array}{c} \sqrt{2}F^+ \\ H^3 + iH^4 \end{array} \right) , \tag{29}$$

with the vacuum expectation values,

$$< \phi_1 >= \frac{1}{\sqrt{2}} \left(\begin{array}{c} 0 \\ v \end{array} \right) \; ; < \phi_2 >= 0 \; ; < \phi_3 >= 0 \; . \tag{30}$$

Note that, the similar choice was done in the literature for the general 2HDM (model III) [25]. The Yukawa interaction responsible for the Flavor Changing (FC) interactions is

$$\mathcal{L}_{Y,FC} = \xi_{ij}^U \bar{Q}_{iL} \tilde{\phi}_2 U_{jR} + \xi_{ij}^D \bar{Q}_{iL} \phi_2 D_{jR} + \rho_{ij}^U \bar{Q}_{iL} \tilde{\phi}_3 U_{jR} + \rho_{ij}^D \bar{Q}_{iL} \phi_3 D_{jR} + h.c. \; . \tag{31}$$

and the couplings $\xi^{U,D}$ and $\rho^{U,D}$ for the charged FC interactions are

$$\begin{aligned} \xi^U_{ch} &= \xi_N \, V_{CKM} \; , \\ \xi^D_{ch} &= V_{CKM} \, \xi_N \; , \\ \rho^U_{ch} &= \rho_N \, V_{CKM} \; , \\ \rho^D_{ch} &= V_{CKM} \, \rho_N \; , \end{aligned} \tag{32}$$

and

$$\begin{aligned} \xi^{U,D}_N &= (V_L^{U,D})^{-1} \xi^{U,D} \, V_R^{U,D} \; , \\ \rho^{U,D}_N &= (V_L^{U,D})^{-1} \rho^{U,D} \, V_R^{U,D} \; , \end{aligned} \tag{33}$$

In the 3HDM model, the Higgs sector is extended and therefore the number of free parameters, namely, masses of new charged and neutral Higgs particles, new Yukawa couplings, increases. Fortunately, by introducing a new transformation in the Higgs sector and taking the 3HDM Lagrangian invariant under it, the number of free parameters can be reduced enormously [18]. Taking the following $O(2)$ transformation:

$$\begin{aligned} \phi_1^{\prime} &= \phi_1 \; , \\ \phi_2^{\prime} &= cos\,\alpha \; \phi_2 + sin\,\alpha \; \phi_3 \; , \\ \phi_3^{\prime} &= -sin\,\alpha \; \phi_2 + cos\,\alpha \; \phi_3 \; , \end{aligned} \tag{34}$$

where α is the global parameter, which represents a rotation of the vectors ϕ_2 and ϕ_3 along the axis where ϕ_1 lies and assuming the invariance of the gauge and CP invariant Higgs potential

$$
\begin{aligned}
V(\phi_1,\phi_2,\phi_3) &= c_1(\phi_1^+\phi_1 - v^2/2)^2 + c_2(\phi_2^+\phi_2)^2 \\
&+ c_3(\phi_3^+\phi_3)^2 + c_4[(\phi_1^+\phi_1 - v^2/2) + \phi_2^+\phi_2 + \phi_3^+\phi_3]^2 \\
&+ c_5[(\phi_1^+\phi_1)(\phi_2^+\phi_2) - (\phi_1^+\phi_2)(\phi_2^+\phi_1)] \\
&+ c_6[(\phi_1^+\phi_1)(\phi_3^+\phi_3) - (\phi_1^+\phi_3)(\phi_3^+\phi_1)] \\
&+ c_7[(\phi_2^+\phi_2)(\phi_3^+\phi_3) - (\phi_2^+\phi_3)(\phi_3^+\phi_2)] \\
&+ c_8[Re(\phi_1^+\phi_2)]^2 + c_9[Re(\phi_1^+\phi_3)]^2 + c_{10}[Re(\phi_2^+\phi_3)]^2 \\
&+ c_{11}[Im(\phi_1^+\phi_2)]^2 + c_{12}[Im(\phi_1^+\phi_3)]^2 + c_{13}[Im(\phi_2^+\phi_3)]^2 + c_{14} \qquad (35)
\end{aligned}
$$

we get the masses of new particles as

$$
\begin{aligned}
m_{F^\pm} &= m_{H^\pm} \ , \\
m_{H^3} &= m_{H^1} \ , \\
m_{H^4} &= m_{H^2} \ ,
\end{aligned} \qquad (36)
$$

Further, the application of this transformation to the Yukawa Lagrangian eq.(28) allows us to write the equality

$$
(\xi'^{U(D)})^+\xi'^{U(D)} + (\rho'^{U(D)})^+\rho'^{U(D)} = (\xi^{U(D)})^+\xi^{U(D)} + (\rho^{U(D)})^+\rho^{U(D)} \ , \qquad (37)
$$

where

$$
\begin{aligned}
\xi'^{U(D)}_{ij} &= \xi^{U(D)}_{ij} cos\,\alpha + \rho^{U(D)}_{ij} sin\,\alpha \ , \\
\rho'^{U(D)}_{ij} &= -\xi^{U(D)}_{ij} sin\,\alpha + \rho^{U(D)}_{ij} cos\,\alpha \ .
\end{aligned} \qquad (38)
$$

and therefore the Yukawa matrices $\xi^{U(D)}$ and $\rho^{U(D)}$ can be parametrized as,

$$
\begin{aligned}
\xi^{U(D)} &= \epsilon^{U(D)} cos\,\theta \ , \\
\rho^{U} &= \epsilon^{U} sin\,\theta \ , \\
\rho^{D} &= i\epsilon^{D} sin\,\theta \ .
\end{aligned} \qquad (39)
$$

Here $\epsilon^{U(D)}$ are real matrices satisfy the equation

$$
(\xi'^{U(D)})^+\xi'^{U(D)} + (\rho'^{U(D)})^+\rho'^{U(D)} = (\epsilon^{U(D)})^T\epsilon^{U(D)} \qquad (40)
$$

and T denotes transpose operation. Finally, we could reduce the number of the Yukawa matrices $\xi^{U,(D)}$ and $\rho^{U,(D)}$, by connecting them with the expression given in eq.(39). Further, we take into account only the Yukawa couplings $\xi^U_{N,tt}$, $\xi^D_{N,bb}$, $\rho^U_{N,tt}$ and $\rho^D_{N,bb}$, since we assume that the others are small due to the discussion given in [20].

C Appendix The operator basis and the Wilson coefficients for the decay $b \to s\gamma\gamma$ in the model III

The operator basis is the same as the one used for the $b \to s\gamma$ decay in the model III [20] and $SU(2)_L \times SU(2)_R \times U(1)$ extensions of the SM [27]:

$$
\begin{aligned}
O_1 &= (\bar{s}_{L\alpha}\gamma_\mu c_{L\beta})(\bar{c}_{L\beta}\gamma^\mu b_{L\alpha}), \\
O_2 &= (\bar{s}_{L\alpha}\gamma_\mu c_{L\alpha})(\bar{c}_{L\beta}\gamma^\mu b_{L\beta}), \\
O_3 &= (\bar{s}_{L\alpha}\gamma_\mu b_{L\alpha}) \sum_{q=u,d,s,c,b} (\bar{q}_{L\beta}\gamma^\mu q_{L\beta}), \\
O_4 &= (\bar{s}_{L\alpha}\gamma_\mu b_{L\beta}) \sum_{q=u,d,s,c,b} (\bar{q}_{L\beta}\gamma^\mu q_{L\alpha}), \\
O_5 &= (\bar{s}_{L\alpha}\gamma_\mu b_{L\alpha}) \sum_{q=u,d,s,c,b} (\bar{q}_{R\beta}\gamma^\mu q_{R\beta}), \\
O_6 &= (\bar{s}_{L\alpha}\gamma_\mu b_{L\beta}) \sum_{q=u,d,s,c,b} (\bar{q}_{R\beta}\gamma^\mu q_{R\alpha}), \\
O_7 &= \frac{e}{16\pi^2}\bar{s}_\alpha\sigma_{\mu\nu}(m_b R + m_s L) b_\alpha \mathcal{F}^{\mu\nu}, \\
O_8 &= \frac{g}{16\pi^2}\bar{s}_\alpha T^a_{\alpha\beta}\sigma_{\mu\nu}(m_b R + m_s L) b_\beta \mathcal{G}^{a\mu\nu} \;, \\
O_9 &= (\bar{s}_{L\alpha}\gamma_\mu c_{L\beta})(\bar{c}_{R\beta}\gamma^\mu b_{R\alpha}), \\
O_{10} &= (\bar{s}_{L\alpha}\gamma_\mu c_{L\alpha})(\bar{c}_{R\beta}\gamma^\mu b_{R\beta}),
\end{aligned} \tag{41}
$$

and the second operator set $O'_1 - O'_{10}$ which are flipped chirality partners of $O_1 - O_{10}$:

$$
\begin{aligned}
O'_1 &= (\bar{s}_{R\alpha}\gamma_\mu c_{R\beta})(\bar{c}_{R\beta}\gamma^\mu b_{R\alpha}), \\
O'_2 &= (\bar{s}_{R\alpha}\gamma_\mu c_{R\alpha})(\bar{c}_{R\beta}\gamma^\mu b_{R\beta}), \\
O'_3 &= (\bar{s}_{R\alpha}\gamma_\mu b_{R\alpha}) \sum_{q=u,d,s,c,b} (\bar{q}_{R\beta}\gamma^\mu q_{R\beta}), \\
O'_4 &= (\bar{s}_{R\alpha}\gamma_\mu b_{R\beta}) \sum_{q=u,d,s,c,b} (\bar{q}_{R\beta}\gamma^\mu q_{R\alpha}), \\
O'_5 &= (\bar{s}_{R\alpha}\gamma_\mu b_{R\alpha}) \sum_{q=u,d,s,c,b} (\bar{q}_{L\beta}\gamma^\mu q_{L\beta}),
\end{aligned}
$$

$$
\begin{aligned}
O'_6 &= (\bar{s}_{R\alpha}\gamma_\mu b_{R\beta}) \sum_{q=u,d,s,c,b} (\bar{q}_{L\beta}\gamma^\mu q_{L\alpha}), \\
O'_7 &= \frac{e}{16\pi^2}\bar{s}_\alpha \sigma_{\mu\nu}(m_b L + m_s R) b_\alpha \mathcal{F}^{\mu\nu}, \\
O'_8 &= \frac{g}{16\pi^2}\bar{s}_\alpha T^a_{\alpha\beta}\sigma_{\mu\nu}(m_b L + m_s R) b_\beta \mathcal{G}^{a\mu\nu}, \\
O'_9 &= (\bar{s}_{R\alpha}\gamma_\mu c_{R\beta})(\bar{c}_{L\beta}\gamma^\mu b_{L\alpha}) \ , \\
O'_{10} &= (\bar{s}_{R\alpha}\gamma_\mu c_{R\alpha})(\bar{c}_{L\beta}\gamma^\mu b_{L\beta}) \ ,
\end{aligned} \tag{42}
$$

where α and β are $SU(3)$ colour indices and $\mathcal{F}^{\mu\nu}$ and $\mathcal{G}^{\mu\nu}$ are the field strength tensors of the electromagnetic and strong interactions, respectively. In the calculations, we take only the charged Higgs contributions into account and neglect the effects of neutral Higgs bosons (see [16] for details). Further, in our expressions we use the redefinition,

$$
\xi^{U,D} = \sqrt{\frac{4G_F}{\sqrt{2}}}\,\bar{\xi}^{U,D} \ . \tag{43}
$$

Denoting the Wilson coefficients for the SM with $C_i^{SM}(m_W)$ and the additional charged Higgs contribution with $C_i^H(m_W)$, we have the initial values for the first set of operators (eq.(41)) ([20] and references within)

$$
\begin{aligned}
C^{SM}_{1,3,\ldots 6,9,10}(m_W) &= 0 \ , \\
C^{SM}_2(m_W) &= 1 \ , \\
C^{SM}_7(m_W) &= \frac{3x^3-2x^2}{4(x-1)^4}\ln x + \frac{-8x^3-5x^2+7x}{24(x-1)^3} \ , \\
C^{SM}_8(m_W) &= -\frac{3x^2}{4(x-1)^4}\ln x + \frac{-x^3+5x^2+2x}{8(x-1)^3} \ , \\
C^{H}_{1,\ldots 6,9,10}(m_W) &= 0 \ , \\
C^{H}_7(m_W) &= \frac{1}{m_t^2}\,(\bar{\xi}^U_{N,tt}+\bar{\xi}^U_{N,tc}\frac{V^*_{cs}}{V^*_{ts}})\,(\bar{\xi}^U_{N,tt}+\bar{\xi}^U_{N,tc}\frac{V_{cb}}{V_{tb}})F_1(y) \ , \\
&+ \frac{1}{m_t m_b}\,(\bar{\xi}^U_{N,tt}+\bar{\xi}^U_{N,tc}\frac{V^*_{cs}}{V^*_{ts}})\,(\bar{\xi}^D_{N,bb}+\bar{\xi}^D_{N,sb}\frac{V_{ts}}{V_{tb}})F_2(y) \ , \\
C^{H}_8(m_W) &= \frac{1}{m_t^2}\,(\bar{\xi}^U_{N,tt}+\bar{\xi}^U_{N,tc}\frac{V^*_{cs}}{V^*_{ts}})\,(\bar{\xi}^U_{N,tt}+\bar{\xi}^U_{N,tc}\frac{V_{cb}}{V_{tb}})G_1(y) \ , \\
&+ \frac{1}{m_t m_b}\,(\bar{\xi}^U_{N,tt}+\bar{\xi}^U_{N,tc}\frac{V^*_{cs}}{V^*_{ts}})\,(\bar{\xi}^D_{N,bb}+\bar{\xi}^U_{N,sb}\frac{V_{ts}}{V_{tb}})G_2(y) \ ,
\end{aligned} \tag{44}
$$

and for the second set of operators eq. (42),

$$
\begin{aligned}
C'^{SM}_{1,\ldots 10}(m_W) &= 0 \ , \\
C'^{H}_{1,\ldots 6,9,10}(m_W) &= 0 \ , \\
C'^{H}_7(m_W) &= \frac{1}{m_t^2}\,(\bar{\xi}^D_{N,bs}\frac{V_{tb}}{V^*_{ts}}+\bar{\xi}^D_{N,ss})\,(\bar{\xi}^D_{N,bb}+\bar{\xi}^D_{N,sb}\frac{V_{ts}}{V_{tb}})F_1(y) \ ,
\end{aligned}
$$

$$
\begin{aligned}
& + \quad \frac{1}{m_t m_b} (\bar{\xi}^D_{N,bs} \frac{V_{tb}}{V^*_{ts}} + \bar{\xi}^D_{N,ss}) (\bar{\xi}^U_{N,tt} + \bar{\xi}^U_{N,tc} \frac{V_{cb}}{V_{tb}}) F_2(y) \; , \\
C'^H_8(m_W) & = \frac{1}{m_t^2} (\bar{\xi}^D_{N,bs} \frac{V_{tb}}{V^*_{ts}} + \bar{\xi}^D_{N,ss}) (\bar{\xi}^D_{N,bb} + \bar{\xi}^D_{N,sb} \frac{V_{ts}}{V_{tb}}) G_1(y) \; , \\
& + \quad \frac{1}{m_t m_b} (\bar{\xi}^D_{N,bs} \frac{V_{tb}}{V^*_{ts}} + \bar{\xi}^D_{N,ss}) (\bar{\xi}^U_{N,tt} + \bar{\xi}^U_{N,tc} \frac{V_{cb}}{V_{tb}}) G_2(y) \; , \qquad (45)
\end{aligned}
$$

where $x = m_t^2/m_W^2$ and $y = m_t^2/m_{H^\pm}^2$. The functions $F_1(y)$, $F_2(y)$, $G_1(y)$ and $G_2(y)$ are given as

$$
\begin{aligned}
F_1(y) & = \frac{y(7-5y-8y^2)}{72(y-1)^3} + \frac{y^2(3y-2)}{12(y-1)^4} \, lny \; , \\
F_2(y) & = \frac{y(5y-3)}{12(y-1)^2} + \frac{y(-3y+2)}{6(y-1)^3} \, lny \; , \\
G_1(y) & = \frac{y(-y^2+5y+2)}{24(y-1)^3} + \frac{-y^2}{4(y-1)^4} \, lny \; , \\
G_2(y) & = \frac{y(y-3)}{4(y-1)^2} + \frac{y}{2(y-1)^3} \, lny \; . \qquad (46)
\end{aligned}
$$

Note that we neglect the contributions of the internal u and c quarks compared to one due to the internal t quark. In the $3HDM(O_2)$ model, the Wilson coefficients are obtained with the replacement $\bar{\xi}^{U(D)} \rightarrow \bar{\epsilon}^{U(D)}$ and the redefinition of λ_θ, $\lambda_\theta = \frac{1}{m_t m_b} \bar{\epsilon}^U_{N,tt} \bar{\epsilon}^D_{N,bb} (cos^2\theta + i\, sin^2\theta)$.

For the initial values of the Wilson coefficients in the model III (eqs. (44)and (45)), we have

$$
\begin{aligned}
C^{2HDM}_{1,3,...6,9,10}(m_W) & = 0 \; , \\
C^{2HDM}_2(m_W) & = 1 \; , \\
C^{2HDM}_7(m_W) & = C^{SM}_7(m_W) + C^H_7(m_W) \; , \\
C^{2HDM}_8(m_W) & = C^{SM}_8(m_W) + C^H_8(m_W) \; , \\
C'^{2HDM}_{1,2,3,...6,9,10}(m_W) & = 0 \; , \\
C'^{2HDM}_7(m_W) & = C'^{SM}_7(m_W) + C'^H_7(m_W) \; , \\
C'^{2HDM}_8(m_W) & = C'^{SM}_8(m_W) + C'^H_8(m_W) \; . \qquad (47)
\end{aligned}
$$

At this stage it is possible to obtain the result for model II, in the approximation $\frac{m_s}{m_b} \sim 0$ and $\frac{m_b^2}{m_t^2} \sim 0$, by making the following replacements in the Wilson coefficients:

$$
\begin{aligned}
\bar{\xi}^{U*}_{st} \bar{\xi}^U_{tb} & = m_t^2 \frac{1}{tan^2\beta} \; , \\
\bar{\xi}^{U*}_{st} \bar{\xi}^D_{tb} & = -m_t m_b \; , \qquad (48)
\end{aligned}
$$

and taking zero for the coefficients of the flipped operator set, i.e $C'_i \rightarrow 0$.

The evaluation of the Wilson coefficients are done by using the initial values $C_i^{2HDM\,(3HDM(O_2)}$ ($C_i'^{2HDM\,(3HDM(O_2))}$) and their contributions at any lower scale can be calculated as in the SM case [20].

D Appendix The necessary functions used in the Wilson coefficients

The explicit forms of the functions $I(m_q)$, $J(m_q)$ and $\triangle(m_q)$ appearing in eqs. 3 and 4 are

$$\begin{aligned}
I(m_q) &= 1 + \frac{m_q^2}{m_{B_s}^2} \triangle(m_q) \, , \\
J(m_q) &= 1 - \frac{m_{B_s}^2 - 4m_q^2}{4m_{B_s}^2} \triangle(m_q) \, , \\
\triangle(m_q) &= \left(\ln(\frac{m_{B_s} + \sqrt{m_{B_s}^2 - 4m_q^2}}{m_{B_s} - \sqrt{m_{B_s}^2 - 4m_q^2}}) - i\pi \right)^2 \;\; \text{for} \;\; \frac{m_{B_s}^2}{4m_q^2} \geq 1, \\
\triangle(m_q) &= - \left(2\arctan(\frac{\sqrt{4m_q^2 - m_{B_s}^2}}{m_{B_s}}) - \pi \right)^2 \;\; \text{for} \;\; \frac{m_{B_s}^2}{4m_q^2} < 1.
\end{aligned} \tag{49}$$

References

[1] J. L. Hewett, in proc. of the 21^{st} Annual SLAC Summer Institute, ed. L. De Porcel and C. Dunwoode, SLAC-PUB6521.

[2] S. Herrlich and J. Kalinowski , Nucl. Phys. B **381** (1992) 501.

[3] L. Reina, G. Ricciardi and A. Soni,Phys. Lett B **396** (1997) 231.

[4] G.-L. Lin, J. Liu and Y.-P. Yao, Phys. Rev. Lett. **64** (1990) 1498;
G.-L. Lin, J. Liu and Y.-P. Yao, Phys. Rev. D **42** (1990) 2314.

[5] H. Simma and D. Wyler, Nucl. Phys. B **344** (1990) 283.

[6] T. M. Aliev and G. Turan, Phys. Rev. D **48** (1993) 1176.

[7] B. Grinstein, R. Springer, and M. Wise, Nucl. Phys. B**339** (1990) 269; R. Grigjanis, P.J. O'Donnel, M. Sutherland and H. Navelet, Phys. Lett. B**213** (1988) 355; Phys. Lett. B**286** (1992) E, 413; G. Cella, G. Curci, G. Ricciardi and A. Viceré, Phys. Lett. B**325** (1994) 227, Nucl. Phys. B**431** (1994) 417; M. Misiak, Nucl. Phys B**393** (1993) 23, Erratum B**439** (1995) 461.

[8] K. G. Chetyrkin, M. Misiak and M. Münz, Phys. Lett.B **400** (1997) 206; C. Greub, T. Hurth and D. Wyler, Phys. Lett.B **380** (1996) 385; Phys. Rev. D **54** (1996) 3350.

[9] M. Ciuchini, E. Franco, G. Martinelli, L. Reina and L. Silvestrini, Phys. Lett. B**316** (1993) 127; Nucl. Phys. B**421** (1994) 41.

[10] A. J. Buras, M. Misiak, M. Münz and S. Pokorski, Nucl. Phys. B**424** (1994) 374.

[11] G. Hiller and E. Iltan, Phys. Lett. B**409** (1997) 425.

[12] C. H. V. Chang, G. L. Lin and Y. P. Yao, Phys. Lett. B**415** (1997) 395.

[13] L. Reina, G. Ricciardi and A. Soni, Phys. Rev. D**56** (1997) 5085.

[14] T. M. Aliev, G. Hiller and E. O. Iltan, Nucl. Phys. B**515** (1998) 321.

[15] S. Bertolini and J. Matias, Phys. Rev. D **57** (1998) 4197.

[16] T. M. Aliev and E. O. Iltan, Phys. Rev. D**58** (1998) 095014 .

[17] M. Acciarri et al. (L3 Collaboration), Phys. Lett. B **363** (1995) 127.

[18] E. Iltan, to appear in Phys. Rev. D, hep-ph/9903202.

[19] M. Ciuchini et al., Nucl. Phys. B**527** (1998) 21.

[20] T. M. Aliev, and E. Iltan, J. Phys. G**25** (1999) 989,

[21] E. Iltan, Phys. Rev. D**60** (1999) 034023.

[22] A. J. Buras and M. Münz, Phys. Rev. D**52** (1995) 186.

[23] G. Hiller and E. O. Iltan, Mod. Phys. Lett. A **12** (1997) 2837.

[24] M. S. Alam et al., CLEO Collaboration, ICHEP 98 Conference,1998

[25] D. Atwood, L. Reina and A. Soni, Phys. Rev. D**55** (1997) 3156.

[26] D. B. Chao, K. Cheung and Keung, hep-ph/98011235 (1998)

[27] P. Cho and Misiak, Phys. Rev. D **49** (1994) 5894.

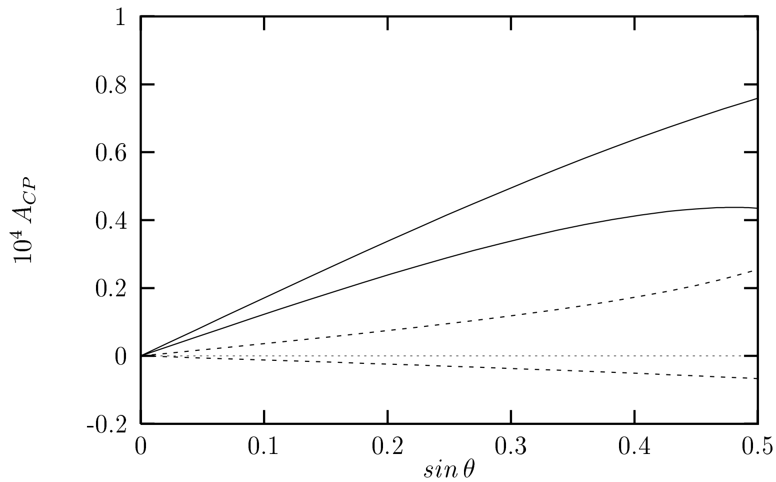

Figure 1: A_{CP} as a function of $sin\,\theta$ for $\bar{\xi}^{D}_{N,bb} = 40\, m_b$ and $m_H^{\pm} = 400\, GeV$ in the region $|r_{tb}| < 1$, at the scale $\mu = m_b/2$, without LD effects, in model III. Here A_{CP} is restricted in the region bounded by solid lines for $C_7^{eff} > 0$ and by dashed lines for $C_7^{eff} < 0$.

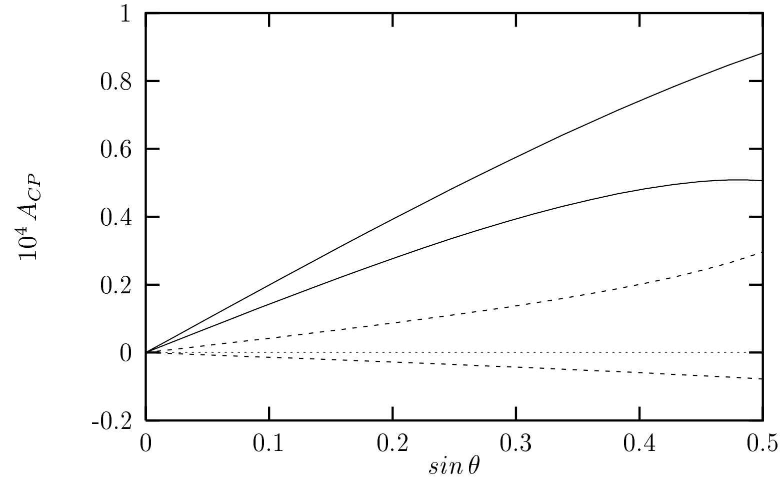

Figure 2: The same as Fig. 1 but with LD effects.

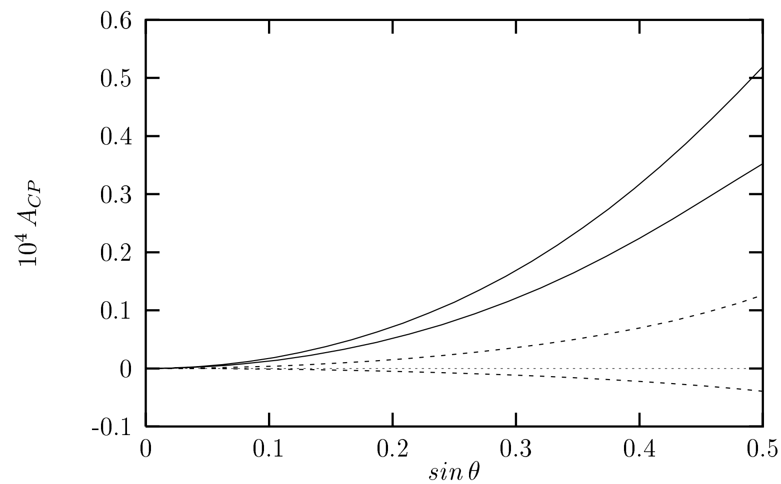

Figure 3: The same as Fig. 1 but for $3HDM(O_2)$ and $\bar{\epsilon}^D_{N,bb} = 40\, m_b$.

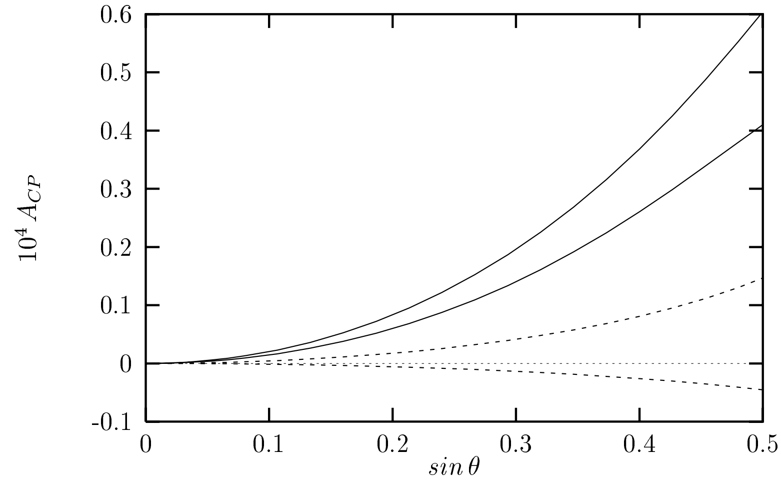

Figure 4: The same as Fig. 3 but with LD effects.

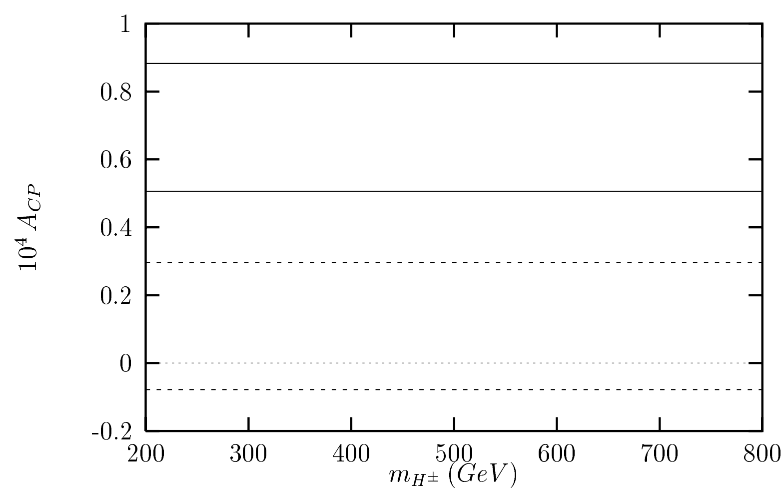

Figure 5: A_{CP} as a function of $m_{H^\pm}$ for $sin\,\theta = 0.5$ and $\bar{\xi}^{D}_{N,bb} = 40\, m_b$ in the region $|r_{tb}| < 1$, at the scale $\mu = m_b/2$, with LD effects, in model III. Here A_{CP} is restricted in the region bounded by solid lines for $C_7^{eff} > 0$ and by dashed lines for $C_7^{eff} < 0$.

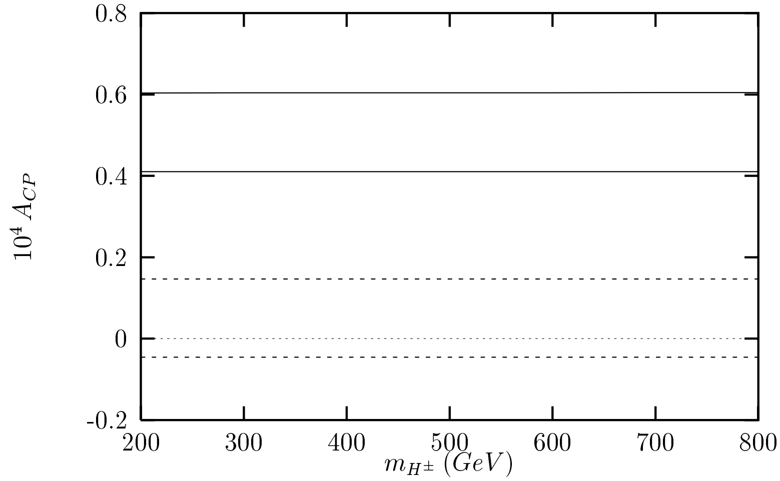

Figure 6: The same as Fig **??**, but for $3HDM(O_2)$ and $\bar{\epsilon}^{D}_{N,bb} = 40\, m_b$.

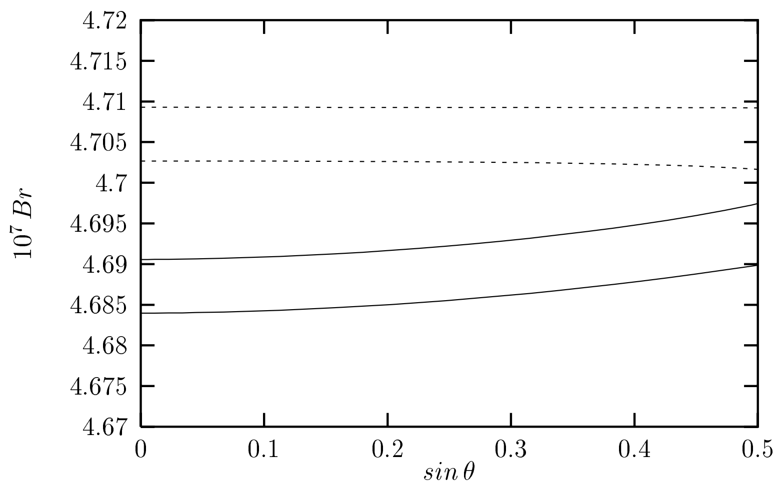

Figure 7: Br as a function of $sin\,\theta$ for $\bar{\xi}^{D}_{N,bb} = 40\, m_b$ and $m_H^{\pm} = 400\, GeV$ in the region $|r_{tb}| < 1$, at the scale $\mu = m_b/2$, without LD effects, in model III. Here Br is restricted in the region bounded by solid lines for $C_7^{eff} > 0$ and by dashed lines for $C_7^{eff} < 0$.

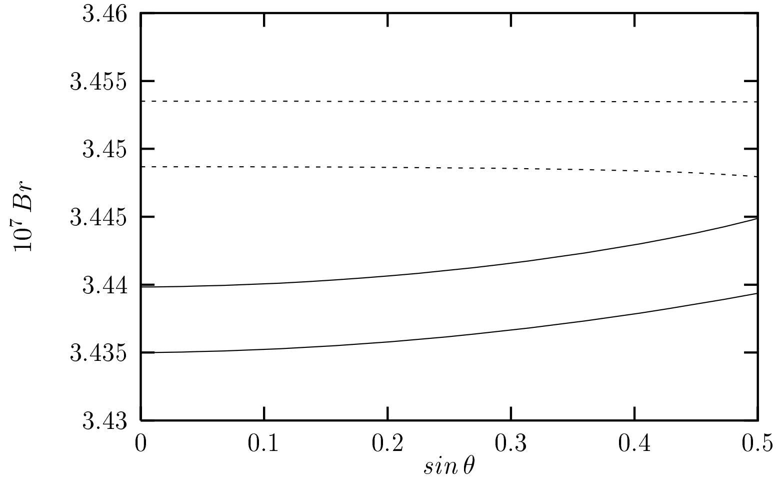

Figure 8: The same as Fig 7, but with LD effects.

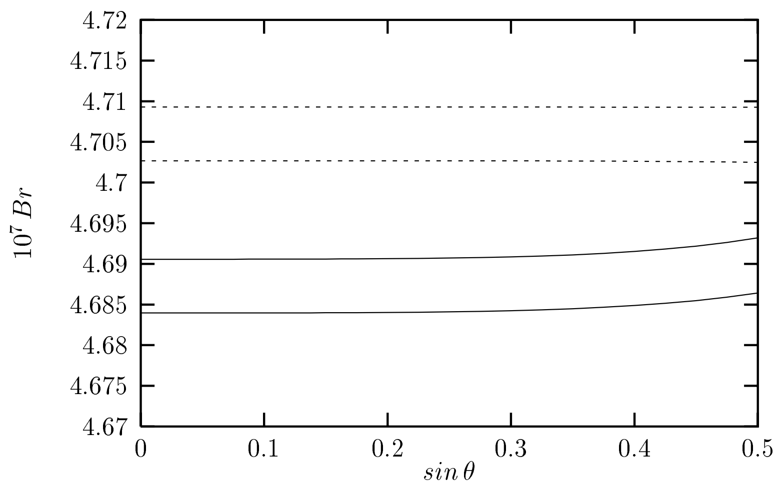

Figure 9: The same as Fig 7, but for $3HDM(O_2)$ and $\bar{\epsilon}^D_{N,bb} = 40\, m_b$.

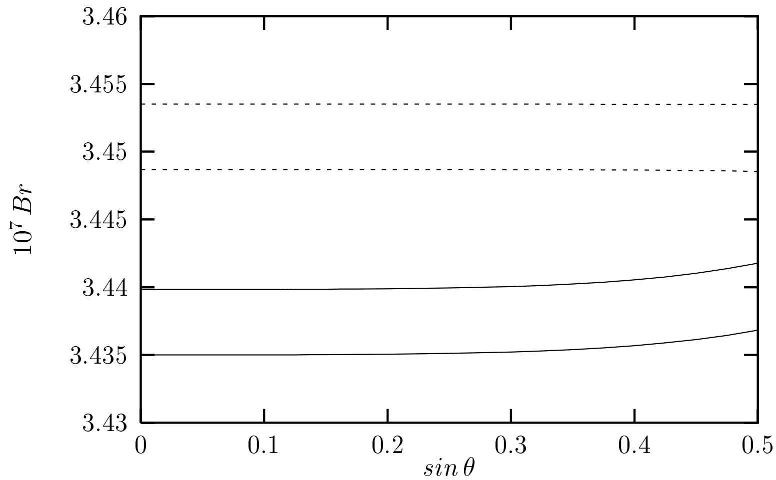

Figure 10: The same as Fig 9, but with LD effects.

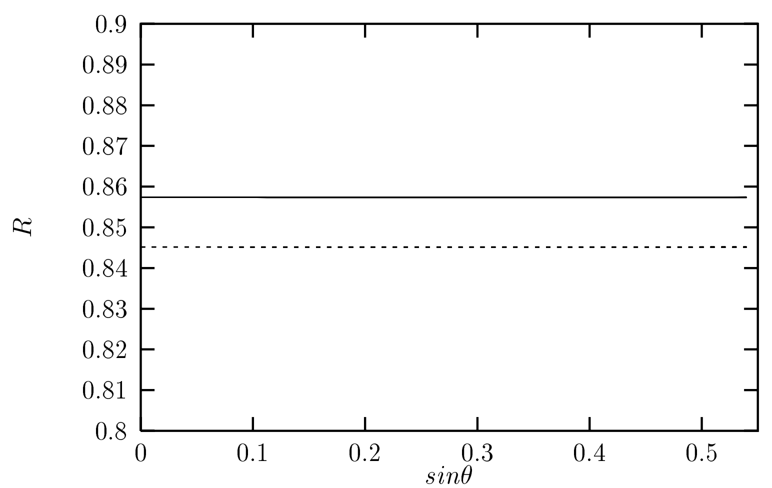

Figure 11: R ratio as a function of $sin\,\theta$ for $\bar{\xi}^{D}_{N,bb} = 40\,m_b$ and $m_H^{\pm} = 400\,GeV$ in the region $|r_{tb}| < 1$, at the scale $\mu = m_b/2$, in model III. Here R ratio is restricted on the solid (dashed) line for $C_7^{eff} > 0$ ($C_7^{eff} < 0$). Note that, for $3HDM(O_2)$, R ratio is almost the same as the one calculated in model III.